

Intracellular Ca^{2+} release via the ER translocon activates store-operated calcium entry

Hwei L. Ong · Xibao Liu · Ajay Sharma ·
Ramanujan S. Hegde · Indu S. Ambudkar

Received: 26 June 2006 / Revised: 2 August 2006 / Accepted: 14 August 2006 / Published online: 14 December 2006
© Springer-Verlag 2006

Abstract Store-operated Ca^{2+} entry (SOCE) is activated in response to depletion of intracellular Ca^{2+} from the endoplasmic reticulum (ER). A variety of agonists stimulate SOCE via IP_3 -dependent Ca^{2+} depletion. SOCE is also activated by thapsigargin, an inhibitor of Ca^{2+} reuptake into the ER that induces a net Ca^{2+} loss from the ER by unmasking a Ca^{2+} “leak” pathway. The molecular identity of this Ca^{2+} leak channel and the physiological conditions under which such agonist-independent Ca^{2+} depletion might occur remain poorly characterized. In this study, we report that inhibition of the initiation step of protein synthesis (with pactamycin) resulted in detectable Ca^{2+} depletion in ER and activation of SOCE. This was completely prevented if the ribosome–nascent chain complexes were first stabilized with an irreversible inhibitor of translational elongation (emetine), suggesting that ER Ca^{2+} depletion had occurred through open translocons at the ER. Notably, emetine pretreatment also attenuated thapsigargin-mediated Ca^{2+} release and SOCE. Furthermore, both pactamycin and thapsigargin stimulated translocation of STIM1, a protein required for activation of

SOCE, to the subplasma membrane region and activated the SOCE-associated current, I_{SOC} . In aggregate, these data reveal an agonist-independent mechanism for internal Ca^{2+} store depletion and activation of SOCE. We suggest that the functional coupling between SOCE and protein synthesis is likely to be critical for maintaining $[\text{Ca}^{2+}]_{\text{ER}}$ within a range that is required to prevent ER stress during changes in cellular translational activity.

Keywords Store-operated Ca^{2+} entry · Endoplasmic reticulum · Ca^{2+} · Pactamycin · Thapsigargin · Translocons

Introduction

Store-operated calcium entry (SOCE) is activated by the depletion of calcium in the endoplasmic reticulum (ER). Physiologically, this is achieved when agonists, such as carbachol, trigger a G protein-mediated activation of phospholipase C pathway, resulting in the breakdown of phosphatidylinositol 4,5-bisphosphate and generation of the second messengers, diacylglycerol and inositol 1,4,5-triphosphate (IP_3). IP_3 then binds to its receptor in the ER membrane and induces calcium release via IP_3 receptor, leading to depletion of the ER calcium store. According to the conformational hypothesis [8, 13], the IP_3 receptor undergoes a conformational change following store depletion which enables it to interact with and activate the plasma membrane store-operated calcium channels (SOCs). This interaction then induces Ca^{2+} influx via the SOCs. Thapsigargin also causes release of intracellular Ca^{2+} from the same IP_3 -sensitive intracellular calcium store, by inhibiting the sarco/endoplasmic reticulum ($\text{Ca}^{2+} + \text{Mg}^{2+}$) ATP-ase (SERCA) pumps in the ER membrane [21, 32].

H. L. Ong · X. Liu · I. S. Ambudkar (✉)
Secretary Physiology Section,
Gene Therapy and Therapeutics Branch,
National Institute of Dental and Craniofacial Research,
Bethesda, MD 20892, USA
e-mail: indu.ambudkar@nih.gov

A. Sharma · R. S. Hegde
Cell Biology and Metabolism Branch,
National Institute of Child Health and Human Development,
National Institutes of Health,
Bethesda, MD 20892, USA

Present address:

I. S. Ambudkar
Building 10, Room 1N-113, 10 Center Drive, NIH,
Bethesda, MD 20892, USA

Thapsigargin-mediated Ca^{2+} store depletion directly activates SOCE without involvement of PIP_2 metabolism. Thus, thapsigargin is widely used to activate SOCE. However, the pathway(s) that mediate thapsigargin-induced Ca^{2+} release from the ER is not yet known. Further, the mechanism(s) by which internal Ca^{2+} store depletion is relayed to the plasma membrane to activate SOCE has not been fully elucidated.

A major channel in the ER is the translocon through which nascent secretory and membrane proteins are translocated. Although the protein-conducting channel in the translocon is a theoretical source of Ca^{2+} leak, it has long been presumed to be tightly gated to preserve the permeability barrier across the ER. A series of biochemical experiments using fluorescent probes has shown that the translocon is impermeable to iodide ions at all stages of protein translocation *in vitro* [1, 9]. It has been suggested that the cytosolic side is blocked by the ribosome during translocation, while the chaperone BiP blocks the luminal side of both active and inactive translocons [7, 10]. Although the role of these interactions has been questioned on the basis of structural studies [34], permeability through the translocon is nonetheless presumed to be tightly regulated to prevent ion leak. However, recent studies have challenged this view. For example, the ER in semipermeabilized cultured mammalian cells was shown to be permeable to a small polar sugar through pores that were blocked during active protein synthesis [26]. Furthermore, premature release of translocating nascent polypeptides with puromycin resulted in detectable ion flux across the membrane *in vitro* [28] and Ca^{2+} leak *in vivo* [3, 20]. However, because puromycin prematurely evacuates the translocons, it may not reflect the events that occur physiologically when a stop codon is reached and peptide synthesis is terminated. Nonetheless, these findings raise the intriguing possibility that translocons which are not actively engaged with substrate are potential sources of Ca^{2+} leak.

Physiologically, at least some proportion of translocons at any time is likely to be empty of substrate. Even under conditions of maximal protein synthesis, empty translocons would exist, at least transiently, upon completion of protein translocation that accompanies translational termination. Thus, luminal Ca^{2+} could conceivably be released into the cytosol during this process. Recent studies demonstrate that puromycin-mediated clearance of the translocon increased the rate of cyclopiazonic acid-induced store depletion via a mechanism that was independent of IP_3 and ryanodine receptors [20, 33]. Thus, it was suggested that Ca^{2+} release induced by inhibition of SERCA pumps is mediated via the translocon complex. However, Ca^{2+} flux via the translocon upon physiological completion of protein synthesis has not been directly

demonstrated and the effect of this release on cellular functions such as SOCE has not been examined.

In this study, we have examined the possible involvement of the translocon in internal Ca^{2+} release and activation of SOCE by using protein synthesis inhibitors that act at different stages of the translation cycle. We present novel data which show that physiological termination of protein synthesis and subsequent completion of protein translocation generates empty translocons that leak Ca^{2+} from the ER and activate SOCE.

Materials and methods

Materials

Thapsigargin was obtained from Calbiochem (San Diego, CA, USA). The FITC-conjugated donkey anti-rabbit antibody was obtained from Jackson ImmunoResearch (West Grove, PA, USA). 2-Aminoethyl-diphenylborinate (2-APB), antimycin A, emetine and oligomycin were obtained from Sigma–Aldrich (St. Louis, MO, USA). ER Tracker Blue–White dye, Fura-2AM, Mag-Fluo4AM were obtained from Molecular Probes (Eugene, OR, USA). Anti-Sec61 β has been described previously [4].

Cell culture

Human salivary gland (HSG) cells were cultured as described previously [19]. Briefly, HSG cells were cultured in Earle's minimal essential medium supplemented with 10% fetal bovine serum, 1% penicillin/streptomycin at 37°C in 5% CO_2 . For $[\text{Ca}^{2+}]_i$ measurements and live cell imaging, confluent cells were detached from tissue culture dishes and plated on glass-bottomed 35 mm tissue culture dishes (MatTek, Ashland, MA, USA). For electrophysiology measurements and immunofluorescence experiments, cells were plated on glass coverslips. Measurements were done after 24 h.

$[\text{Ca}^{2+}]_i$ measurements

Measurements were conducted as described previously [19]. Briefly, cells grown in glass-bottomed 35 mm dishes were loaded with 1 μM Fura-2AM for 1 h at 37°C in 5% CO_2 . Fluorescence measurements in single cells were acquired using a Till Photonics–Polychrome IV spectrofluorimeter attached to Olympus X51 inverted microscope (OPELCO, Dulles, VA, USA) and CoolSnap HQ camera (Roper Scientific, Tuscon, AZ, USA) with Metamorph Imaging Software (Molecular Devices, Sunnyvale, CA, USA). Additions of various compounds, including 1 mM CaCl_2 , were made as shown in the figures. Analog plots of

the average fluorescence ratio (340/380 nm) are shown. Origin 6 (Microcal, Northampton, MA, USA) was used for analyses of data.

Electrophysiological measurements

Cell-attached patch clamp measurements were performed as described previously [16, 29]. Briefly, coverslips were transferred to the recording chamber and kept in a Ringer's solution [in mM: 145 NaCl, 5 KCl, 1 MgCl₂, 1 CaCl₂, 10 4-(2-Hydroxyethyl)-1-piperazineethanesulfonic acid (HEPES), 10 glucose; pH 7.4 NaOH]. The patch pipette had resistances between 3–5 mΩ after filling with the standard intracellular solution (in mM: 145 cesium methane-sulfonate, 8 NaCl, 10 MgCl₂, 10 HEPES, 10 ethyleneglycotetraacetic acid; pH 7.2 CsOH). External solutions were composed as follows (in mM): 145 NaCl, 5 CsCl, 1 MgCl₂, 10 CaCl₂, 10 HEPES, 10 glucose; pH 7.4 NaOH). Osmolality for all the solution was adjusted with mannose to 300 to 315 mmol/kg using Vapor Pressure Osmometer (Wescor, Logan, UT, USA). Patch-clamp experiments were performed in the tight-seal whole cell configuration at room temperature (22–25°C) using Axon-patch 200B amplifier (Molecular Devices). The development of the current was assessed by measuring the current amplitudes at a potential of –70 mV, taken from high resolution currents in response to voltage ramps ranging from –90 to 90 mV over a period of 1 s for every 4 s, and digitized at a rate of 1 KHz. A liquid-junction potential of less than 8 mV was not corrected and capacitive currents and series resistance were determined and minimized. For analysis, the first ramp was used for leak subtraction of the subsequent current records. P-Clamp 7 (Molecular Devices) and Origin 6 (Microcal) were used for analyses of data.

Analyses of the ribosome–translocon association

Cultured HSG cells were either treated with pactamycin or thapsigargin or left untreated for 5 min at 37°C. Lysates from HSG cells were then prepared as described previously [30]. Briefly, whole cell lysates were centrifuged through a 10–50% sucrose gradient and 200 μl fractions were sequentially removed from the centrifuged lysate. These fractions were then pooled together into light, medium, and heavy fractions. Immunoblotting using the anti-Sec61β antibody was carried out as described previously [30].

In vitro translation of calreticulin

cDNA encoding a green fluorescent protein (GFP) fusion of calreticulin (Crt-GFP) was transcribed and translated in vitro using a rabbit reticulocyte lysate translation system [27]. The indicated protein synthesis inhibitors (pactamycin

at 400 nM; emetine at 10 μM; puromycin at 200 μM) were added to the translation reactions at either 0 or 5 min, and the reactions were allowed to continue for an additional 30 min. Immunoblotting using the anticalreticulin antibody was carried out as described previously [27].

Immunofluorescence and confocal imaging

Immunofluorescence was conducted in a similar manner as described previously [2], but with the addition of 50 μg/ml RNase A to the blocking solution. Cells were stained with the rabbit anti-Sec61β (1:1,000) [30] and probed using a donkey anti-rabbit antibody conjugated to FITC (1:100). Fluorescence images were acquired using a confocal laser scanning microscope Leica TCS-SP2 attached to an upright Leica DM-RE7 microscope as described earlier [2]. Details of the images are indicated in the figure and text.

Live cells imaging using the ER Tracker Blue–White dye

Cells were loaded with 0.5 μM ER Tracker Blue–White dye at 37°C for 30 min and immediately viewed using a Till Photonics–Polychrome IV spectrofluorimeter attached to Olympus X51 inverted microscope and CoolSnap HQ camera (Roper Scientific) and Metamorph Imaging Software (Molecular Devices).

[Ca²⁺]_{ER} measurements

HSG cells were plated overnight in glass-bottom dishes and loaded with 3 μM Mag-Fluo4AM in a similar manner as described previously for the loading of Fura-2AM [16, 29]. Briefly, cells were loaded with 3 μM Mag-Fluo4AM in culture medium for 1 h at 37°C in a 5% CO₂ incubator. Cells were then used for live cell imaging experiments using the confocal system described above. Pactamycin was added to the cells at 400 nM. To measure fluorescence intensity, cells were scanned in XY-time mode with 10 s increments between each scans. The data points were then normalized and plotted as a measure of fluorescence intensity (units) against time (s).

HSG cell transfection and TIRF microscopy imaging

HSG cells were cultured on glass coverslips and were transiently transfected with YFP-STIM1 (1 μg) for 48 h using the method described previously [18]. The glass coverslip formed the base of a perfusion chamber that was mounted on the stage of an Olympus IX81 motorized inverted microscope (OPELCO). Cells were bathed in a Ca²⁺-containing standard extracellular solution (in mM): 145 NaCl, 5 CsCl, 1 MgCl₂, 10 CaCl₂, 10 HEPES, 10 glucose, pH 7.4 (NaOH) [17]. Solution changes were accomplished by

selecting flow from a multichambered valve-controlled mechanical fed reservoir. Excitation light was provided by a 20-mW Argon Krypton laser. The 488 nm laser was directed into an Olympus TIRF illuminator attached to the rear port of the microscope and through a 488 band pass filter (BP 10 nm) to a TIRF-optimized Olympus Plan APO x60 (1.45 NA) oil immersion objective. Emitted light was collected through a 525-band pass filter (BP 50 nm). Images were collected every 0.5 s using a Hamamatsu EM C9100 backthinned camera (512 × 512; Hamamatsu, Tokyo, Japan) controlled using the Openlab modular imaging software (Synergy Software, Reading, PA, USA).

Results

Pactamycin activates SOCE

Several previous studies [20, 33] have demonstrated that premature release of nascent peptide chains from ribosomes with puromycin to abruptly vacate engaged translocons (see Fig. 1a) results in Ca^{2+} release from the ER, a result that we have also confirmed (data not shown). However, it was unclear from such studies whether the Ca^{2+} leak was due to artificially vacated translocons and whether empty translocons generated upon physiological termination of protein synthesis would be similarly permeable to Ca^{2+} . To investigate whether empty translocons are involved in Ca^{2+} leak from the ER, and therefore activation of SOCE, we examined the effects of the protein synthesis inhibitor, pactamycin, on HSG cells. Pactamycin inhibits protein synthesis at the initiation step preventing assembly of the ribosome-translocon channel complex (see Fig. 1a). Hence, ribosomes already engaged on mRNAs are allowed to continue polypeptide synthesis normally and complete translation upon reaching the termination codon. As the nascent polypeptides complete their synthesis translocons are converted from an engaged to an empty state. To confirm the effects of pactamycin, emetine, and puromycin on mammalian protein synthesis, the effects of these inhibitors on the translation of Crt-GFP were investigated. Note that pactamycin inhibits synthesis of Crt-GFP completely only when added at the beginning of the reaction, but not after 5 min (Fig. 1b). By contrast, both emetine and puromycin inhibit protein synthesis completely irrespective of time of addition (Fig. 1b). These findings are indicative of pactamycin being a selective inhibitor of translational initiation in the mammalian system at this concentration because elongation can proceed normally in its presence. By contrast, both emetine and puromycin effectively inhibit elongation by either locking nascent chains in the ribosome (emetine) or eliciting their premature release (puromycin). The asterisk indicates the position of hemoglobin, a

background band often observed in reticulocyte lysate (Fig. 1b).

Treatment of HSG cells with pactamycin at concentrations used to inhibit protein synthesis induced no detectable increase in $[\text{Ca}^{2+}]_i$ in the absence of external

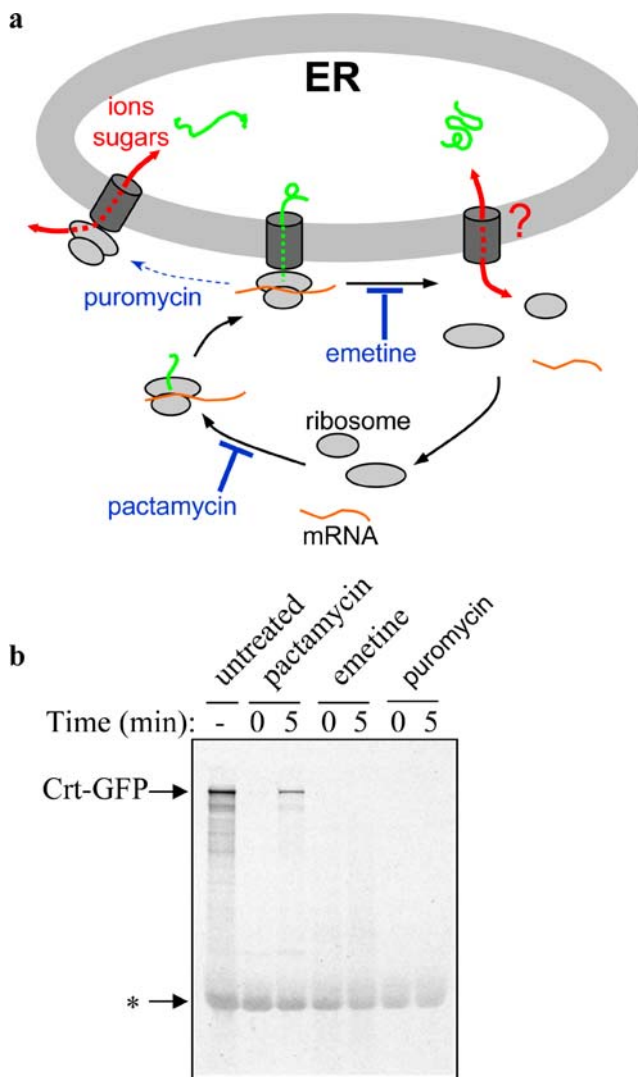


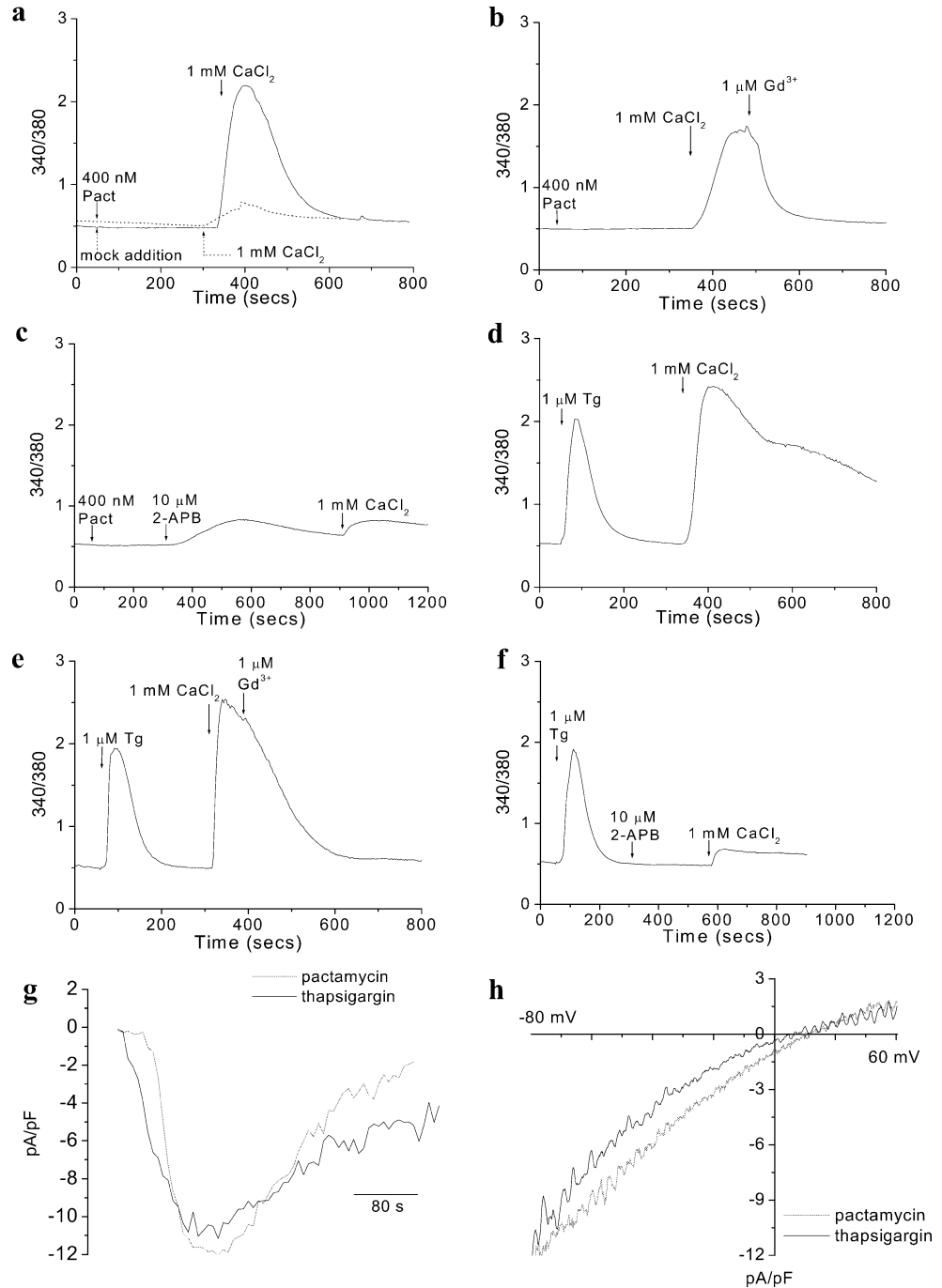
Fig. 1 Site of inhibitor actions on protein translation and translocation. **a** The translation cycle begins with ribosome assembly on the mRNA and initiation of polypeptide synthesis (*bottom diagram*). Ribosomes synthesizing secretory and membrane proteins are targeted to translocons (*gray cylinders*) at the ER membrane, where translocation occurs cotranslationally (*middle diagram*). Upon completion of translation, the translocon returns to its inactive state (*right diagram*). Translocation can be aborted prematurely by release of nascent polypeptides with puromycin (*left diagram*), a state shown previously to be conducive of ions and sugars across the ER membrane. Emetine inhibits elongation of translation by the ribosome, thereby stalling translocons in their engaged and active state. Pactamycin, by inhibiting initiation of translation, allows all translocating polypeptides to complete their synthesis normally and converts the translocons to their physiologically inactive state. **b** Effect of the protein synthesis inhibitors on GFP-calreticulin synthesis using a reticulocyte lysate system. Inhibitors were added either at time “0” (before the reaction was started) or after 5 min of reaction. Other details are provided in the figure and in the “Materials and methods” section

Ca^{2+} . However, readdition of Ca^{2+} to the medium induced substantial $[\text{Ca}^{2+}]_i$ increase (Fig. 2a, solid line; dotted line indicates basal Ca^{2+} entry in untreated cells). Longer incubation with pactamycin (15 min and 30 min) did not change this pattern (data not shown). This Ca^{2+} influx was blocked by the addition of $1 \mu\text{M Gd}^{3+}$ or $10 \mu\text{M 2-APB}$ to the external medium (Fig. 2b,c, respectively; addition of $1 \mu\text{M Gd}^{3+}$ to cells before readdition of Ca^{2+} induced similar block of Ca^{2+} entry, data not shown). Ca^{2+} entry induced by thapsigargin (Fig. 2d) was also blocked by $1 \mu\text{M Gd}^{3+}$ and $10 \mu\text{M 2-APB}$ (Fig. 2e,f, respectively). Thus, like thapsi-

gargin, pactamycin treatment of cells results in activation of store-operated Ca^{2+} entry. However, $[\text{Ca}^{2+}]_i$ increase in pactamycin-treated cells appeared to be more transient than in thapsigargin-treated cells (compare Fig. 2a,d). The faster inactivation seen with pactamycin may be due to Ca^{2+} reuptake into the ER by SERCA pumps, which are still active in these cells but not in those treated with thapsigargin.

Activation of store-operated Ca^{2+} entry by pactamycin was further confirmed by whole cell patch clamp measurements. Pactamycin induced a relatively inwardly rectifying

Fig. 2 Thapsigargin- and pactamycin-induced Ca^{2+} release, Ca^{2+} entry, and Ca^{2+} currents in HSG cells. **a–c** HSG cells were treated with pactamycin (*Pact*) (400 nM) in Ca^{2+} free medium. Ca^{2+} was readded where indicated to control cells (**a**) or after addition of $1 \mu\text{M Gd}^{3+}$ (**b**) or $10 \mu\text{M 2-APB}$ (**c**). Addition of buffer in place of pactamycin induced a much smaller entry but no release. **d–f** Thapsigargin (*Tg*) induced both Ca^{2+} release and entry. $1 \mu\text{M GdCl}_3$ (Gd^{3+} , **e**) and $10 \mu\text{M 2-APB}$ (**f**) inhibited thapsigargin-induced Ca^{2+} entry. **g** Activation of inwardly rectifying cation currents by thapsigargin (*black*) and pactamycin (*gray*). **h** Current–voltage relationship of macroscopic currents induced by thapsigargin and pactamycin. Each analog plot showing Ca^{2+} release and Ca^{2+} entry is representative of at least four experiments, with each trace showing the average for at least 50 cells. Analog plots showing channel events and current–voltage is representative of at least three experiments, with each trace showing the plot obtained with a single cell



current (Fig. 2g,h), which was similar to the thapsigargin-induced store-operated current, I_{SOC} , that we have described in previous studies with HSG cells [16, 29]. In addition, pactamycin also induced similar 2-APB-sensitive Ca^{2+} entry in RBL cells (data not shown). These data demonstrate that pactamycin treatment of cells leads to activation of store-operated Ca^{2+} entry.

Pactamycin induces internal Ca^{2+} store depletion

We initially hypothesized that pactamycin might induce a very small or slow release of Ca^{2+} from the ER and that mitochondrial Ca^{2+} accumulation could prevent a significant increase in $[Ca^{2+}]_i$. However, preincubating cells with a combination of oligomycin (2 μ M) and antimycin A (10 μ M) for 5 min at 37°C did not yield any measurable increase in $[Ca^{2+}]_i$ after pactamycin addition to cells (Fig. 3a), although Ca^{2+} entry appeared to be somewhat decreased. The latter effect of mitochondrial inhibitors on SOCE has been previously reported [22]. Increasing the incubation time with mitochondrial inhibitors to 10 min did not change this observation (data not shown). Thus, lack of detectable internal Ca^{2+} release by pactamycin is likely not due to buffering of cytosolic Ca^{2+} by local mitochondrial Ca^{2+} uptake. Next, we treated cells with high $[La^{3+}]$ to block the plasma membrane Ca^{2+} pump, as previously reported [14]. As shown in Fig. 3b, the inhibition of Ca^{2+} extrusion via the plasma membrane Ca^{2+} pump revealed a gradual increase in $[Ca^{2+}]_i$ in pactamycin-treated cells. These data indicate that pactamycin induces Ca^{2+} release from the ER and suggest that Ca^{2+} extrusion dampens the rise in cytosolic Ca^{2+} . SERCA-dependent recycling of Ca^{2+} back into the ER is also likely to contribute to the lack of $[Ca^{2+}]_i$ increase in pactamycin-treated cells.

To confirm the depletion of internal Ca^{2+} stores by pactamycin, we directly measured $[Ca^{2+}]$ within the ER lumen by using Mag-Fluo4. As shown in Fig. 3c, pactamycin induced a 15% decrease in Mag-Fluo4 fluorescence in the ER, indicating a decrease in luminal $[Ca^{2+}]$. This decrease was significantly greater ($p < 0.025$, $n = 11$ cells) than the basal Ca^{2+} leak from the ER in untreated cells incubated in a Ca^{2+} -free medium ($n = 9$ cells). Thapsigargin (1 μ M) induced a larger and faster decrease (about 50%) in ER Ca^{2+} under the same conditions (data not shown). These data confirm that pactamycin induces Ca^{2+} release from the ER. Lack of detectable increase in cytosolic $[Ca^{2+}]$ is due to pumping of Ca^{2+} back into the ER and extrusion from the cells.

Pactamycin induces depletion of IP_3 -sensitive Ca^{2+} store

We have shown previously that Tg- and carbachol-sensitive internal Ca^{2+} stores overlap in HSG cells [16, 19, 29]. More

importantly, depletion of this store activates SOCE. To determine whether pactamycin acts on the same internal Ca^{2+} store, we examined its effect on carbachol-stimulated Ca^{2+} release and Ca^{2+} entry. One hundred micromolar carbachol induced robust Ca^{2+} release, which was not significantly affected by prior addition of pactamycin

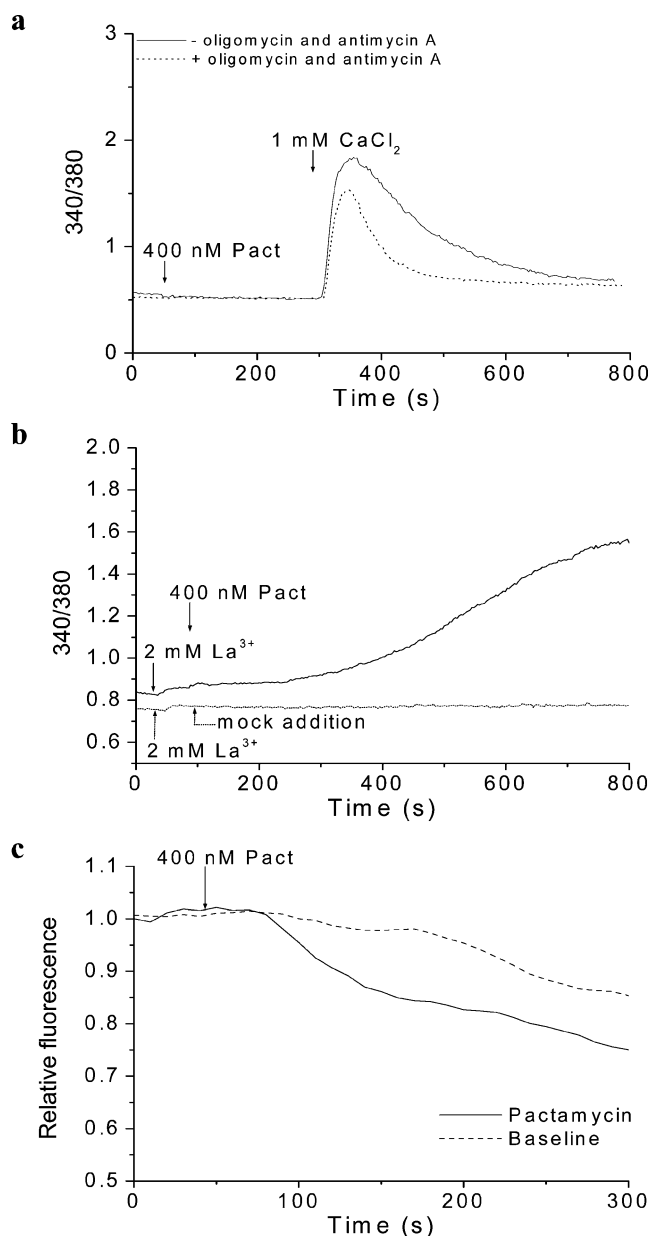


Fig. 3 Pectamycin-induced Ca^{2+} release from the ER. **a** Cells were pretreated with mitochondrial inhibitors, oligomycin (2 μ M), and antimycin A (10 μ M) before addition of pactamycin. **b** 2 mM $LaCl_3$ (La^{3+}) was added to cells to block Ca^{2+} extrusion via the plasma membrane Ca^{2+} pumps before addition of pactamycin. **c** Cells were loaded with Mag-Fluo 4 and changes in ER- Ca^{2+} was detected by monitoring fluorescence in pactamycin-treated cells (data with thapsigargin are not shown). Each analog plot is representative of at least three experiments, with each trace showing the average for at least 20 cells

(Fig. 4a,b). However, $[Ca^{2+}]_i$ increase was more sustained ($P < 0.001$, see average data in Fig. 4f) in these cells although the rate of influx was not changed. Consistent with the data shown in Fig. 3, preincubating the cells with 400 nM pactamycin for longer time periods (data with 15 min preincubation are shown in the figure) completely abolished carbachol-induced Ca^{2+} release and slightly reduced Ca^{2+} influx (Fig. 4c). Increasing preincubation time with pactamycin to 30 min further reduced Ca^{2+} influx (data not shown). These data further confirm our observation that pactamycin treatment induces depletion of internal Ca^{2+} stores. This is further illustrated in subpanels d–h of Fig. 4 which show the effects of pactamycin on 1 μ M carbachol-

induced Ca^{2+}_i changes. Measurements in single cells demonstrate robust $[Ca^{2+}]_i$ oscillations (Fig. 4g,h), average $[Ca^{2+}]_i$ changes from ≥ 50 cells are shown in Fig. 4d,e. Addition of pactamycin before carbachol did not significantly decrease internal Ca^{2+} release (compare Fig. 4d,e). However, as was the case with higher [carbachol], the magnitude of influx was significantly ($P < 0.001$) increased (Fig. 4d,e). Importantly, addition of pactamycin during the oscillations induced by 1 μ M carbachol rapidly inhibited further oscillations (Fig. 4h). These data demonstrate that pactamycin acts on the same Ca^{2+} store as carbachol. We suggest that (1) the more sustained Ca^{2+} entry seen upon carbachol stimulation of cells pretreated with pactamycin is

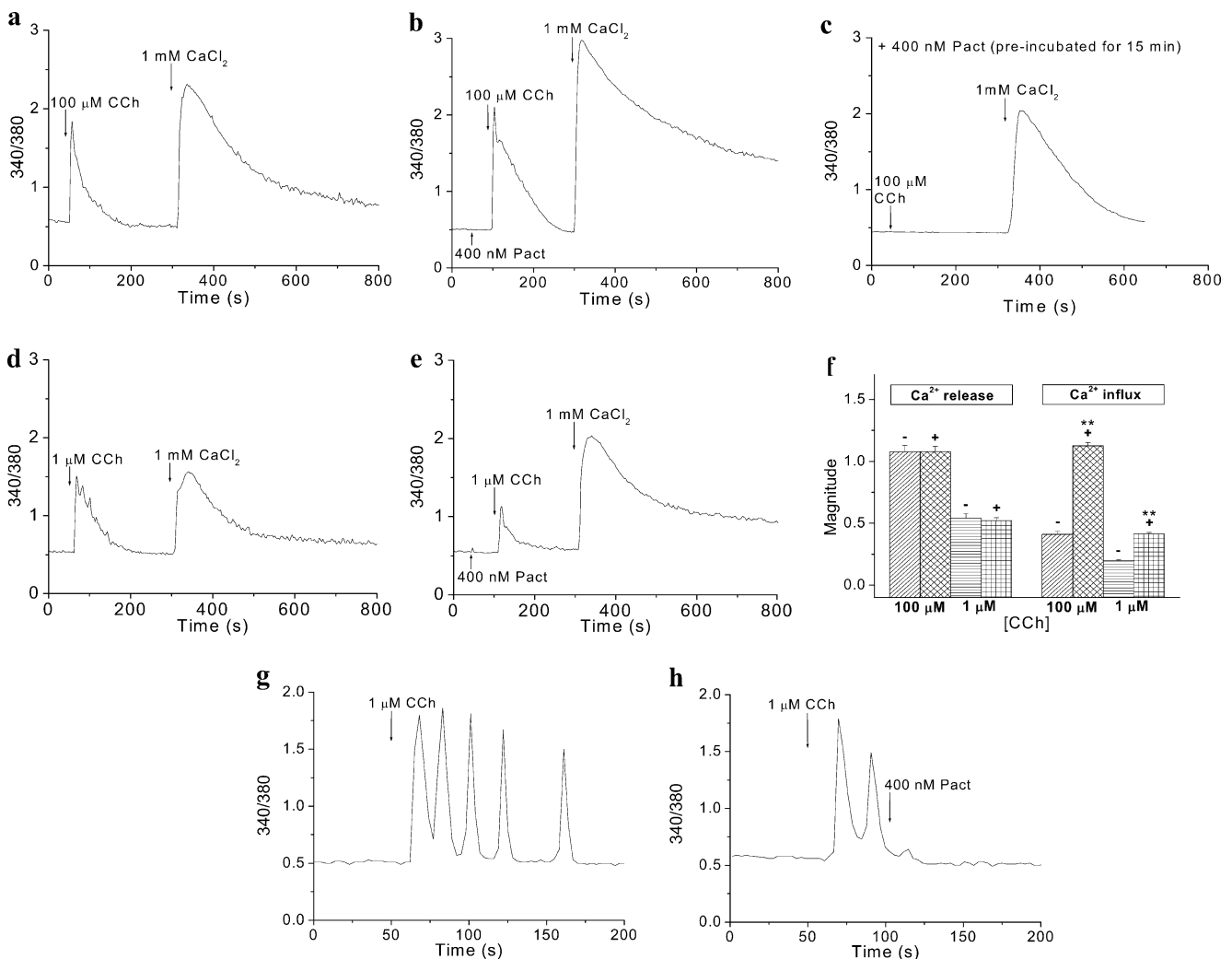


Fig. 4 Effects of pactamycin on carbachol-induced Ca^{2+} release and Ca^{2+} entry. **a, b** Carbachol (CCh; 100 μ M)-induced Ca^{2+} release and Ca^{2+} entry in the (a) absence and (b) presence of pactamycin (Pact, 400 nM). (c) Carbachol (CCh; 100 μ M)-induced Ca^{2+} release and Ca^{2+} entry after preincubation with pactamycin (Pact, 400 nM) for 15 min. Carbachol (1 μ M)-induced Ca^{2+} release and Ca^{2+} entry in the (d) absence and (e) presence of pactamycin (Pact, 400 nM). **f** Histogram showing the effect of Pact on the magnitude of Ca^{2+} release and Ca^{2+} entry induced by carbachol (100 and 1 μ M). Each

bar column represents mean \pm SEM of data from at least 70 cells. Minus sign indicates that carbachol was added in the absence of pactamycin, whereas plus sign indicates that carbachol was added in the presence of pactamycin. $**P < 0.001$. **g** Oscillatory Ca^{2+} release induced by 1 μ M carbachol. **h** Inhibition of carbachol-stimulated oscillatory Ca^{2+} release by pactamycin (Pact, 400 nM). Each analog plot showing Ca^{2+} release and Ca^{2+} entry is representative of at least four experiments, with each trace showing the average for at least 50 cells

due to block of recycling of Ca^{2+} from cytosol into the ER lumen, thus allowing more complete depletion of the store; and (2) inhibition of carbachol-induced $[\text{Ca}^{2+}]_i$ oscillations and Ca^{2+} release is due to generation of an ER leak.

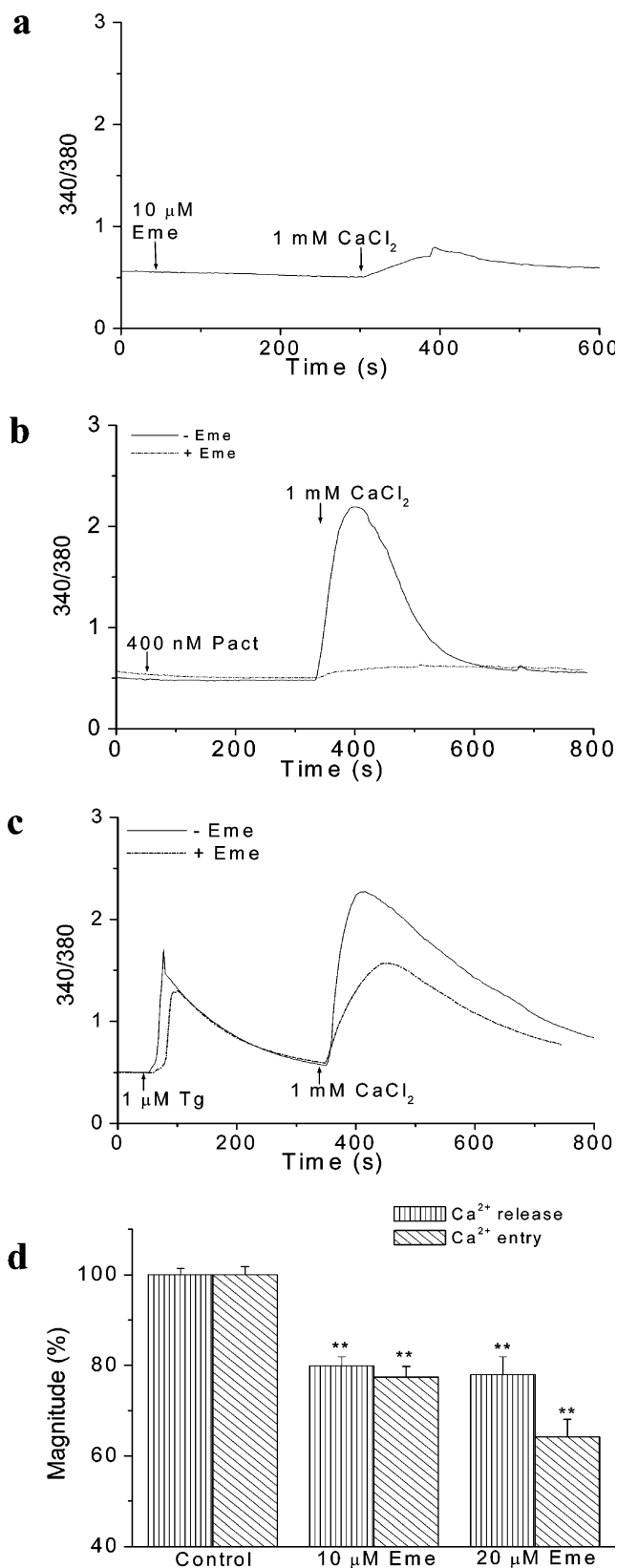
Effect of the ribosome–translocon complex stabilization on activation of SOCE

To address whether the effect of pactamycin on SOCE is mediated through empty translocons generated upon completion of protein synthesis, we analyzed the effect of emetine pretreatment on the ER Ca^{2+} leak. Emetine inhibits protein synthesis by irreversibly preventing elongation of the peptide chain (see Fig. 1). This results in stalled ribosome–nascent chain complexes, which in the case of secretory and membrane proteins results in stably engaged translocons. Emetine alone did not induce any change in $[\text{Ca}^{2+}]_i$ in HSG cells (Fig. 5a). However, preincubation of cells with 10 μM emetine for 5 min at 37°C completely blocked the Ca^{2+} entry induced by pactamycin (Fig. 5b). Importantly, emetine pretreatment also attenuated thapsigargin-induced Ca^{2+} release by 20% ($P < 0.001$, $n \geq 100$ cells) and Ca^{2+} influx by 23% ($P < 0.001$, $n \geq 100$ cells) (Fig. 5c,d). Increasing the incubation time to 10 min and the concentration of emetine to 20 μM did not induce any further decrease in the Ca^{2+} release but did further decrease Ca^{2+} influx ($P < 0.001$, $n \geq 70$ cells) (Fig. 5d).

These data suggest that the effects of pactamycin on Ca^{2+} entry were not induced nonspecifically or as consequence solely of protein synthesis inhibition per se. Rather, pactamycin-mediated SOCE appears to involve the generation of empty translocons as a consequence of termination, an event that can be preempted by first treating with emetine. In addition, and consistent with previous reports [20, 26], these data suggest that the ribosome–translocon complex is involved in thapsigargin-stimulated internal Ca^{2+} release. Loss of SERCA pump activity resulting in decreased reuptake of Ca^{2+} into the ER can, at least in part, account for the weaker effect of emetine on thapsigargin-stimulated $[\text{Ca}^{2+}]_i$ changes. Further, preexisting empty translocons which are likely not affected by emetine will also contribute to this leak.

Fig. 5 Inhibition of pactamycin- and thapsigargin-induced Ca^{2+} release and Ca^{2+} entry by emetine. **a** Effect of emetine (*Eme*) on $[\text{Ca}^{2+}]_i$ in HSG cells. **b** Inhibition of pactamycin (*Pact*)-induced Ca^{2+} entry by 10 μM emetine. **c** Inhibition of thapsigargin (*Tg*)-induced Ca^{2+} release and Ca^{2+} entry by 10 μM emetine. Cells were treated with 10 or 20 μM emetine for 5 min at 37°C prior addition of thapsigargin in **b** and **c**. Each analog plot showing Ca^{2+} release and Ca^{2+} entry is representative of at least three experiments, with each trace showing the average for at least 50 cells. **d** Histogram comparing the Ca^{2+} release (vertical stripes) and Ca^{2+} entry (slanted stripes) (%) induced by thapsigargin in untreated (control) cells and in cells preincubated with 10 or 20 μM emetine. Each bar represents mean \pm SEM of at least 70 cells. ** $P < 0.001$

To confirm these suggestions, we examined the status of translocon engagement in cells treated with pactamycin and thapsigargin. Translocons engaged with substrate are bound



to ribosomes in a salt-resistant manner and can be recovered from the heavy fractions of a sucrose gradient of cell lysates [30]. The light, medium, and heavy fractions (l, m, and h, respectively) were prepared from cells treated with pactamycin or thapsigargin and blotted for the core translocon component Sec61 β . After 5 min of pactamycin treatment, Sec61 β shifted from the heavy to the light/medium fractions relative to untreated control cells (Fig. 6a). This demonstrates that the number of engaged translocons decreases upon acute treatment with pactamycin. Similar results were obtained with lysates of cells treated with thapsigargin for 5 or 30 min. These data are consistent with pactamycin inducing inhibition of protein synthesis (at the initiation step) within minutes [23, 24, 35]. Thus, both thapsigargin and pactamycin result in the generation of a greater number of empty translocons at the ER very shortly after treatment. Subpanels b and c of Fig. 6 show localization of translocon (using anti-Sec61 β antibody) and ER (using live ER tracker dye). Both show reticulate pattern of labeling that is distributed across the cytosol of the cell.

Effect of thapsigargin and pactamycin on STIM1 protein localization

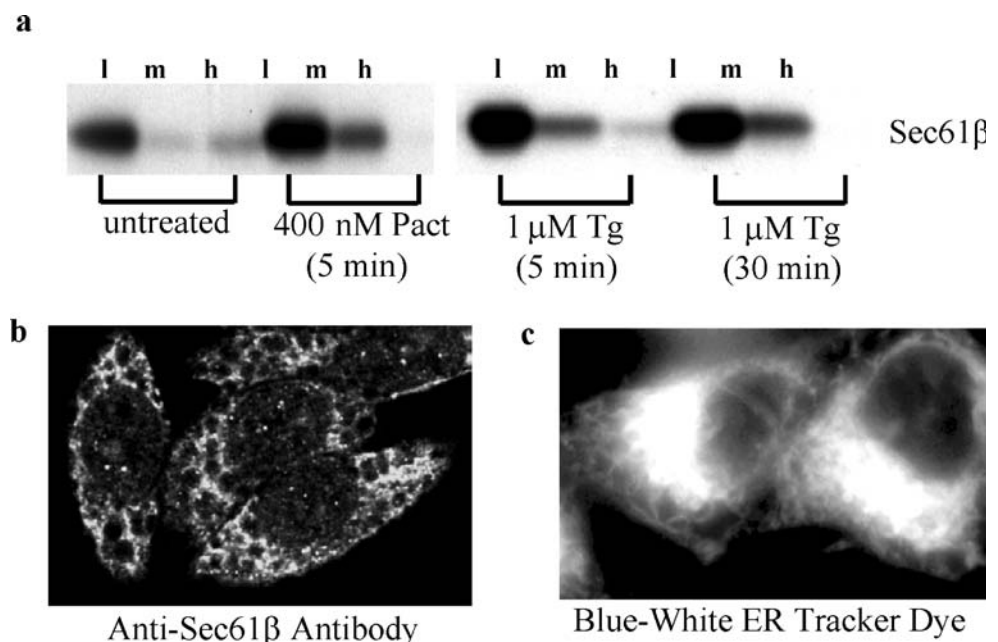
STIM1, an ER Ca²⁺ sensor, has been reported to be required for thapsigargin-mediated activation of SOCE [15, 25, 31, 36]. It was shown that after Ca²⁺ store depletion by thapsigargin, STIM1 is translocated into the plasma membrane region of cells where it appears to have a punctate localization [15, 36]. Consistent with these studies, we have observed that transfection of HSG cells with STIM1 siRNA blocked thapsigargin-induced activation of

SOCE as well as I_{SOC} (Ong et al., unpublished observations). Thus, to further examine the regulation of SOCE by pactamycin, we examined changes in localization of STIM1. HSG cells were transiently transfected with YFP-STIM1 cDNA and translocation of YFP-STIM1 was observed using TIRF microscopy, after stimulation with thapsigargin and pactamycin at concentrations that activate SOCE in HSG cells (see data above). Both thapsigargin and pactamycin induced the translocation of YFP-STIM1 into the plasma membrane (Fig. 7a,b, respectively), although translocation was observed to be slower in the presence of pactamycin. These data provide further evidence that termination of protein synthesis alters the ER-Ca²⁺ status, leading to activation of SOCE.

Discussion

The data presented above demonstrate that the Ca²⁺ leak pathway unmasked by thapsigargin-induced inhibition of the SERCA pump is associated, at least in part, with empty translocon complexes. Further, we show that modulation of the status of the ribosome–translocon complex can influence Ca²⁺ “leak” from the ER. Emetine, which stabilizes the translocon in the engaged state, partially inhibited thapsigargin-stimulated internal Ca²⁺ release. By contrast, increasing the number of empty translocons using pactamycin caused depletion of the internal Ca²⁺ store which was completely prevented by pretreatment with emetine. Pactamycin treatment also significantly attenuated carbachol-stimulated internal Ca²⁺ release and [Ca²⁺]_i oscillations. In aggregate, these data suggest that in its unengaged state, the translocon is permeable to Ca²⁺. More importantly, we show that these

Fig. 6 Dissociation of the ribosome–translocon complex by pactamycin and thapsigargin. **a** Western blot showing the various states of the ribosome–translocon complexes in untreated, pactamycin-treated, and thapsigargin-treated cells. The light (l), medium (m), and heavy (h) fractions are as indicated. Immunoblotting was conducted anti-Sec61 β (1:1,000 dilution) antibody. **b** Confocal imaging showing the localization of Sec61 β protein using the anti-Sec61 β (1:1,000 dilution) antibody in HSG cells. **c** Live cell imaging of ER networks using the ER Tracker Blue–White dye in HSG cells



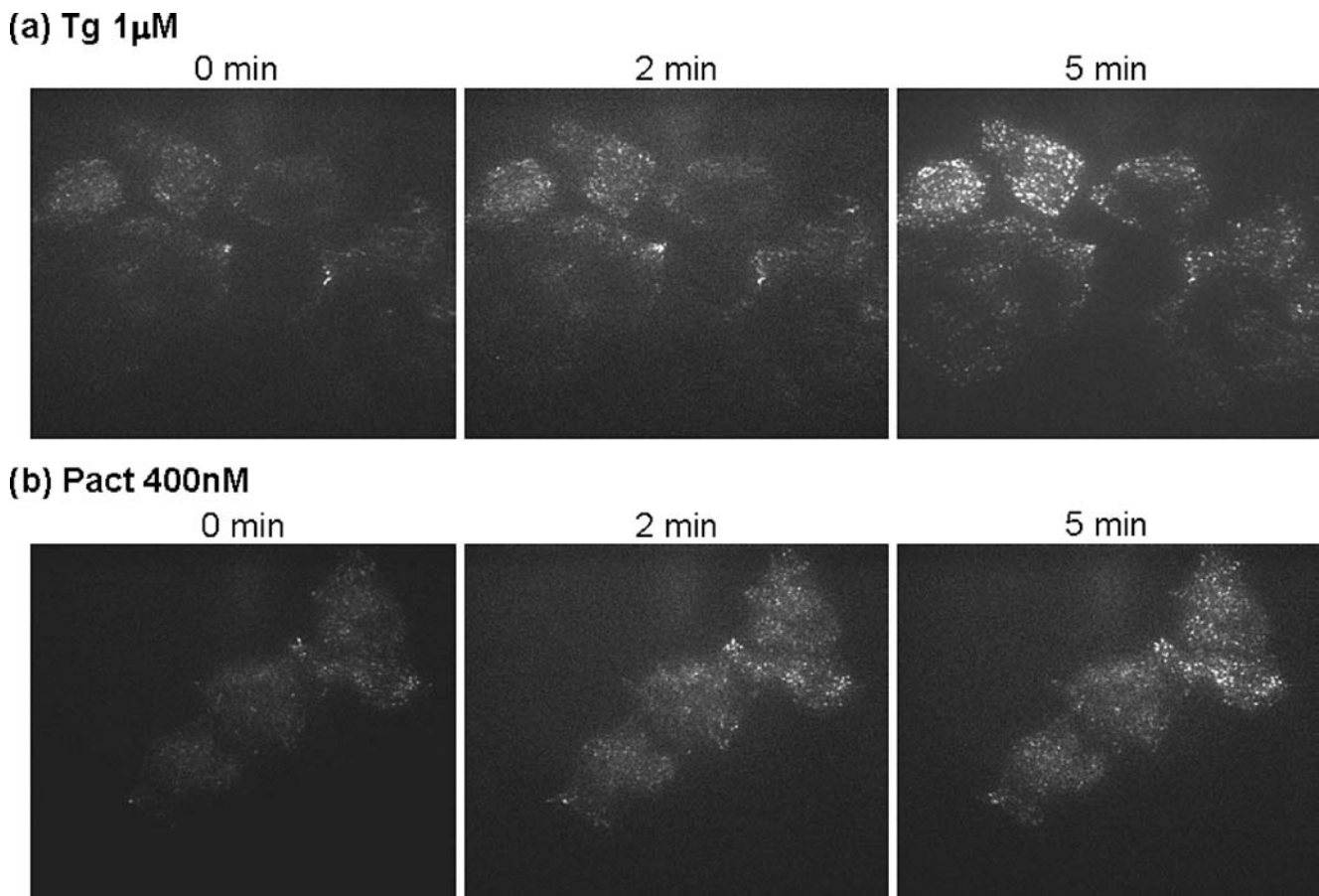


Fig. 7 Thapsigargin and pactamycin cause redistribution of YFP-STIM1. HSG cells were transiently transfected with YFP-STIM1 cDNA. TIRF was used to image localization of STIM1 in the

subplasma membrane region of the cells. Cells were stimulated with (a) thapsigargin (*Tg*; 1 μ M) and (b) pactamycin (*Pact*; 400 nM)

manipulations induce corresponding effects on SOCE. Both pactamycin and thapsigargin activated similar calcium entry that was blocked by 1 μ M Gd^{3+} and 10 μ M 2-APB. Additionally, pactamycin activated a current that was similar to the thapsigargin-induced store-operated current, I_{SOC} . The addition of thapsigargin to pactamycin treated cells did not induce additional currents or Ca^{2+} entry (data not shown). Another significant finding of this study was that pactamycin, like thapsigargin, induced translocation of the SOCE-regulatory protein, STIM1, into the subplasma membrane region.

Possible direct effects of pactamycin on SOCE are ruled out by the inhibition of pactamycin-stimulated Ca^{2+} entry by emetine. Differences in the effects of pactamycin and thapsigargin on $[Ca^{2+}]_i$ were (1) the relatively undetectable $[Ca^{2+}]_i$ increase due to internal Ca^{2+} release in pactamycin-treated cells; and (2) relatively transient $[Ca^{2+}]_i$ increase upon readdition of Ca^{2+} to cells treated with pactamycin in Ca^{2+} -free medium. We suggest that these are due to differences in SERCA-dependent Ca^{2+} recycling ability

and PMCA activity under these two conditions. However, and more importantly, despite lack of detectable “global” $[Ca^{2+}]_i$ increase due to intracellular Ca^{2+} release, our data directly demonstrate that pactamycin depletes ER Ca^{2+} stores. In aggregate, our data show convergent effects of pactamycin and thapsigargin on internal Ca^{2+} store depletion and activation of store-operated Ca^{2+} entry.

These significant findings reveal an agonist-independent mechanism for depletion of internal Ca^{2+} stores and activation of SOCE. We show that clearing of the translocon pore induces release of Ca^{2+} from the internal Ca^{2+} store(s) and activation of SOCE. Under physiological conditions, such clearing of the translocon pore occurs after termination of protein synthesis and release of the nascent peptide. We propose that Ca^{2+} can be released from the ER during this process, although such depletion maybe somewhat transient due to binding of ER lumen chaperones such as BiP to the translocon [12] as well as Ca^{2+} reaccumulation by SERCA activity. The mechanism by which BiP closes the ribosome-free pore is not known.

However, our data suggest that translocon sealing, whether by BiP or by another mechanism, is not absolute and can have a significant role in modulating ER Ca^{2+} permeability.

Although it is presently unclear exactly how much Ca^{2+} release from the ER is required for activation of SOCE, several studies show that SOCE can be activated by submaximal depletion of internal Ca^{2+} stores [5, 6, 11]. Thus, depending upon the rate of protein turnover, sufficient Ca^{2+} could be lost from the ER during termination of protein synthesis to activate SOCE. This link between SOCE and the protein synthesis provides a mechanism whereby the $[\text{Ca}^{2+}]$ in the ER can be maintained at levels optimal for protein folding and maturation in the ER. This will also be critical for protecting the cells against ER stress and activation of the unfolded protein response that result from loss of ER- Ca^{2+} . While it has been well established that SOCE-dependent refilling internal Ca^{2+} stores provides ER- Ca^{2+} for regulation of cellular functions that are mediated by agonist stimulation of PIP_2 hydrolysis, the present data demonstrate a novel agonist-independent, but physiologically critical, cellular function that is associated with ER- Ca^{2+} and SOCE.

Acknowledgements We would like to thank Dr. Tobias Meyer (Department of Molecular Pharmacology, Stanford University) for kindly providing the YFP-STIM1 cDNA. We are also grateful to Dr. Vincent Schram (NICHD, NIH) and Dr. James T. Russell (NICHD, NIH) for their assistance in TIRF microscopy, which was performed at the Microscopy and Imaging Core (NICHD, NIH). We thank Dr. William Swaim for his assistance with the confocal imaging.

References

1. Alder NN, Shen Y, Brodsky JL, Hendershot LM, Johnson AE (2005) The molecular mechanisms underlying BiP-mediated gating of the Sec61 translocon of the endoplasmic reticulum. *J Cell Biol* 168:389–399
2. Bandyopadhyay BC, Swaim WD, Liu X, Redman RS, Patterson RL, Ambudkar IS (2005) Apical localization of a functional TRPC3/TRPC6- Ca^{2+} -signaling complex in polarized epithelial cells. Role in apical Ca^{2+} influx. *J Biol Chem* 280:12908–12916
3. Camello C, Lomax R, Petersen OH, Tepikin AV (2002) Calcium leak from intracellular stores—the enigma of calcium signalling. *Cell Calcium* 32:355–361
4. Fons RD, Bogert BA, Hegde RS (2003) Substrate-specific function of the translocon-associated protein complex during translocation across the ER membrane. *J Cell Biol* 160:529–539
5. Glitsch MD, Parekh AB (2000) Ca^{2+} store dynamics determines the pattern of activation of the store-operated Ca^{2+} current I (CRAC) in response to InsP_3 in rat basophilic leukaemia cells. *J Physiol* 523 (Pt 2):283–290
6. Gutierrez-Martin Y, Martin-Romero FJ, Henao F (2005) Store-operated calcium entry in differentiated C2C12 skeletal muscle cells. *Biochim Biophys Acta* 1711:33–40
7. Haigh NG, Johnson AE (2002) A new role for BiP: closing the aqueous translocon pore during protein integration into the ER membrane. *J Cell Biol* 156:261–270
8. Hamada K, Miyata T, Mayanagi K, Hirota J, Mikoshiba K (2002) Two-state conformational changes in inositol 2,4,5-trisphosphate receptor regulated by calcium. *J Biol Chem* 277:21115–21118
9. Hamman BD, Chen JC, Johnson EE, Johnson AE (1997) The aqueous pore through the translocon has a diameter of 40–60 Å during cotranslational protein translocation at the ER membrane. *Cell* 89:535–544
10. Hamman BD, Hendershot LM, Johnson AE (1998) BiP maintains the permeability barrier of the ER membrane by sealing the luminal end of the translocon pore before and early in translocation. *Cell* 92:747–758
11. Hofer AM, Fasolato C, Pozzan T (1998) Capacitative Ca^{2+} entry is closely linked to the filling state of intercal Ca^{2+} stores: a study using simultaneous measurements of ICRAC and intraluminal $[\text{Ca}^{2+}]_i$. *J Cell Biol* 140:325–334
12. Johnson AE, van Waes MA (1999) The translocon: a dynamic gateway at the ER membrane. *Annu Rev Cell Dev Biol* 15:799–842
13. Kiselyov KI, Shin DM, Wang Y, Pessah IN, Allen PD, Muallem S (2000) Gating of store-operated channels by conformational coupling to ryanodine receptors. *Mol Cell* 6:421–431
14. Kwan CY, Takemura H, Obie JF, Thastrup O, Putney JW Jr (1990) Effects of MeCh, thapsigargin, and La^{3+} on plasmalemmal and intracellular Ca^{2+} transport in lacrimal acinar cells. *Am J Physiol* 258:C1006–C1015
15. Liou J, Kim ML, Heo WD, Jones JT, Myers JW, Ferrell JE Jr, Meyer T (2005) STIM is a Ca^{2+} sensor essential for Ca^{2+} -store-depletion-triggered Ca^{2+} influx. *Curr Biol* 15:1235–1241
16. Liu X, Ambudkar IS (2001) Characteristics of a store-operated calcium-permeable channel. *J Biol Chem* 276:29891–29898
17. Liu X, Singh BB, Ambudkar IS (1999) ATP-dependent activation of KCa and ROMK-type KATP channels in human submandibular gland ductal cells. *J Biol Chem* 274:25121–25129
18. Liu X, Singh BB, Ambudkar IS (2003) TRPC1 is required for functional store-operated Ca^{2+} channels. Role of acidic amino acid residues in the S5-S6 region. *J Biol Chem* 278:11337–11343
19. Liu X, Wang W, Singh BB, Lockwich T, Jadlowiec J, O'Connell B, Wellner R, Zhu MX, Ambudkar IS (2000) Trp1, a candidate protein for the store-operated Ca^{2+} influx mechanisms in salivary gland cells. *J Biol Chem* 275:3403–3411
20. Lomax R, Camello C, Coppenolle FV, Petersen OH, Tepikin AV (2002) Basal and physiological Ca^{2+} leak from the endoplasmic reticulum of pancreatic acinar cells. *J Biol Chem* 277:26479–26485
21. Lytton J, Westlin M, Hanley MR (1991) Thapsigargin inhibits the sarcoplasmic or endoplasmic reticulum Ca-ATPase family of calcium pumps. *J Biol Chem* 266:17067–17071
22. Malli R, Frieden M, Osibow K, Zoratti C, Mayer M, Demareux N, Graier WF (2003) Sustained Ca^{2+} transfer across mitochondria is essential for mitochondrial Ca^{2+} buffering, store-operated Ca^{2+} entry, and Ca^{2+} store refilling. *J Biol Chem* 278:44769–44779
23. Mengesdorf T, Althausen S, Oberdorfer I, Paschen W (2001) Response of neurons to an irreversible inhibition of endoplasmic reticulum Ca(2+)-ATPase: relationship between global protein synthesis and expression and translation of individual genes. *Biochem J* 356:805–812
24. Paschen W, Doutheil J, Gissel C, Treiman M (1996) Depletion of neuronal endoplasmic reticulum calcium stores by thapsigargin: effect on protein synthesis. *J Neurochem* 67:1735–1743
25. Roos J, DiGregorio PJ, Yeromin AV, Ohlsen K, Lioudyno M, Zhang S, Safrina O, Kozak JA, Wagner SL, Cahalan MD, Velicelebi G, Stauderman KA (2005) STIM1, an essential and conserved component of store-operated Ca^{2+} channel function. *J Cell Biol* 169:435–445

26. Roy A, Wonderlin WF (2003) The permeability of the endoplasmic reticulum is dynamically coupled to protein synthesis. *J Biol Chem* 278:4397–4403
27. Shaffer KL, Sharma A, Snapp EL, Hegde RS (2005) Regulation of protein compartmentalization expands the diversity of protein function. *Dev Cell* 9:545–554
28. Simon SM, Blobel G (1991) A protein-conducting channel in the endoplasmic reticulum. *Cell* 65:371–380
29. Singh BB, Liu X, Tang J, Zhu MX, Ambudkar IS (2002) Calmodulin regulates Ca^{2+} -dependent feedback inhibition of store-operated Ca^{2+} influx by interaction with a site in the C terminus of TrpC1. *Mol Cell* 9:739–750
30. Snapp EL, Reinhart GA, Bogert BA, Lippincott-Schwartz J, Hegde RS (2004) The organization of engaged and quiescent translocons in the endoplasmic reticulum of mammalian cells. *J Cell Biol* 164:997–1007
31. Spassova MA, Soboloff J, He LP, Xu W, Dziadek MA, Gill DL (2006) STIM1 has a plasma membrane role in the activation of store-operated Ca^{2+} channels. *Proc Natl Acad Sci USA* 103:4040–4045
32. Thastrup O, Cullen PJ, Drobak BK, Hanley MR, Dawson AP (1990) Thapsigargin, a tumor promoter, discharges intracellular Ca^{2+} stores by specific inhibition of the endoplasmic reticulum Ca^{2+} -ATPase. *Proc Natl Acad Sci USA* 87:2466–2470
33. Van Coppenolle F, Abeele FV, Slomianny C, Flourakis M, Hesketh J, Dewailly E, Prevarskaya N (2004) Ribosome–translocon complex mediates calcium leakage from endoplasmic reticulum stores. *J Cell Sci* 117:4135–4142
34. Van den Berg B, Clemons WM Jr, Collinson I, Modis Y, Hartmann E, Harrison SC, Rapoport TA (2004) X-ray structure of a protein-conducting channel. *Nature* 427:36–44
35. Wong WL, Brostrom MA, Kuznetsov G, Gmitter-Yellen D, Brostrom CO (1993) Inhibition of protein synthesis and early protein processing by thapsigargin in cultured cells. *Biochem J* 289 (Pt 1):71–79
36. Zhang SL, Yu Y, Roos J, Kozak JA, Deerinck TJ, Ellisman MH, Stauderman KA, Cahalan MD (2005) STIM1 is a Ca^{2+} sensor that activates CRAC channels and migrates from the Ca^{2+} store to the plasma membrane. *Nature* 437:902–905